

Hyperfine Structure in the Infrared Spectrum of HD⁺†

Roger D. Ray and Phillip R. Certain

*Theoretical Chemistry Institute and Department of Chemistry, University of Wisconsin-Madison,
Madison, Wisconsin 53706*

(Received 11 February 1977)

The hyperfine structure of the vibration-rotation transitions of HD⁺ is calculated to an accuracy of ± 0.5 MHz. The theoretical spectra confirm the experimental observation that only lines near the center of each transition are intense enough to be detected by the present experiments. The complete spectrum is some 1500 MHz wide and contains structure which has not yet been resolved.

In an elegant beam experiment,¹ Wing, Ruff, Lamb, and Spezeski have observed the infrared spectrum of HD⁺ with resolution sufficient to resolve partially the hyperfine structure of the observed vibration-rotation (v, N)-(v', N') transitions. Bishop has subsequently calculated the band centers of the transitions with an accuracy of ± 0.02 cm⁻¹, and obtained good agreement with experiment.² The purpose of this Letter is to report our calculations of the hyperfine structure of the bands.

The effective Hamiltonian which we used for HD⁺ is

$$H_{\text{eff}} = b_1 \vec{I}_1 \cdot \vec{S} + c_1 I_{1z} S_z + b_2 \vec{I}_2 \cdot \vec{S} + c_2 I_{2z} S_z + \gamma \vec{S} \cdot \vec{N}. \quad (1)$$

Here 1 labels the proton and 2 labels the deuteron. The operators have their usual significance; and the spectroscopic constants, whose calculation is described below, are specific to each rotation-vibration state. Additional terms, such as the nuclear-spin-molecular-rotation interaction and the nuclear spin-spin interaction, have been omitted since their contributions are smaller than the accuracy of the included effects.³ The present experiments do not resolve these smaller contributions either.

The spectroscopic constants are averages of the corresponding electronic functions $b(R)$, $c(R)$, and $\gamma(R)$ over vibration-rotation wave functions.⁴ To within overall scale factors, the same functions are applicable to all isotopic variants of H₂⁺. Although a few calculated vibrational averages have been reported previously⁴⁻⁷ for H₂⁺, the electronic functions, except for the first-order part of $\gamma(R)$, either have not been reported or have not been reported with sufficient accuracy for our purposes. Thus we have repeated the calculation of the electronic functions at a number of closely spaced internuclear separations R . The $b(R)$ and $c(R)$ were obtained by two-dimen-

sional numerical integration using the exact ground-state electronic wave function. The $\gamma(R)$ can be resolved⁴ into the sum of a first-order part γ' and a second-order part γ'' . We calculated the $\gamma'(R)$ by numerical integration and obtained agreement with Luke's tabulation.⁵ We obtained the $\gamma''(R)$ by a perturbation-variation calculation using a large Gaussian lobe basis set for both the unperturbed and perturbed wave functions. The vibration-rotation wave functions and averages were obtained by numerical integration using the adiabatic potential of Bishop and Wetmore.³ Representative results are given in Table I. It is significant that the variation of b_1 with (v, N) is an appreciable fraction of γ . Thus the hyperfine splittings cannot be simply interpreted.

As a check on our calculations, we evaluated the spectroscopic constants for H₂⁺ and compared them with previous calculations and with those derived experimentally.³ The constants b and c have been calculated many times, but only for the (0, 1) state. We obtain 880.50 and 128.23 MHz, compared with the most recently reported results⁵ of 880.7 and 128.5 MHz, respectively. The vibrational averages of b and c given in Table II have

TABLE I. Spectroscopic constants of HD⁺ in MHz. See Eq. (1). $b_2 = r b_1$; $c_2 = r c_1$; $r = g_d/g_p = 0.15351$.

State (v, N)	b_1	c_1	γ
(0, 0)	883.28	129.13	32.06
(0, 1)	882.54	128.91	31.98
(0, 2)	881.04	128.47	31.84
(1, 0)	864.43	121.98	30.35
(1, 1)	863.72	121.76	30.28
(2, 0)	846.87	115.32	28.71
(2, 1)	846.20	115.11	28.64
(2, 2)	844.88	114.70	28.51
(3, 1)	829.91	108.65	27.07
(3, 2)	828.65	108.26	26.94

TABLE II. Spectroscopic constants for H_2^+ in MHz.

v	b	$N=1$		$N=2$	
		c	γ	γ	γ
4	804.48(0.42) ^a	97.96(-0.07)	32.65(0.01)	32.44(0.03) ^b	
5	789.27(0.42)	91.07(-0.11)	30.46(0.04)	30.27(0.06)	
6	775.45(0.44)	84.44(-0.10)	28.27(0.01)	28.09(0.03)	
7	762.95(0.46)	78.07(-0.00)	26.16(0.01)	25.98(0.03)	
8	751.75(0.48)	71.69(-0.04)	24.08(0.00)	23.94(0.05)	

^aValues in parentheses give difference between present values and the experimentally derived constants of Ref. 3.

^bThe values in parentheses give the difference between the present values and the previously calculated values of Ref. 5 and 6.

not been reported in the literature previously. The spin-rotation constant γ has been calculated previously for $(v, N=2)$ states of H_2^+ , and these calculations are compared with our results in Table II. Table II also shows that our constants differ by less than 0.1% from the experimental ones. This same level of agreement may be expected to carry over to the HD^+ constants.

Using the constants in Table I, we diagonalized the spin Hamiltonian H_{eff} and computed the theoretical spectrum for a number of transitions. The result for the $(1,1)-(0,2)$ transition is shown as the "stick" spectrum in Fig. 1. There are many additional lines which are not shown because their intensities are too small to be detected by the present experiments; in particular, there are low-intensity lines displaced 1020 and 370 MHz to higher and lower frequencies, respectively. It is clear that the observed lines contain a number of hyperfine components, as suggested by the experiments.¹

In order to simulate the observed spectrum, we

gave each line a Gaussian line shape with a half-width of 6.5 MHz, which is the experimental Doppler breadth.¹ The true line shape is actually much more complicated than this, and varies from line to line due to saturation effects. Nevertheless, for the reported $(1,1)-(0,2)$ transition, the experimental and calculated splittings are 30 and 30.5 MHz, respectively. A more detailed comparison of theory and experiment must await further analysis of resolution and line-shape problems.

These calculations have shown that, while the present experimental results are an outstanding achievement, further richness in the spectrum will be revealed by subsequent improvements in the experimental resolution.

The authors wish to acknowledge helpful conversations with William H. Wing, Joseph J. Spezeski, R. Claude Woods, and John E. Harriman. They also thank James J. Tortorelli and Thomas A. Dixon for help in checking the calculations, Professor Wing and Dr. Spezeski for sending them

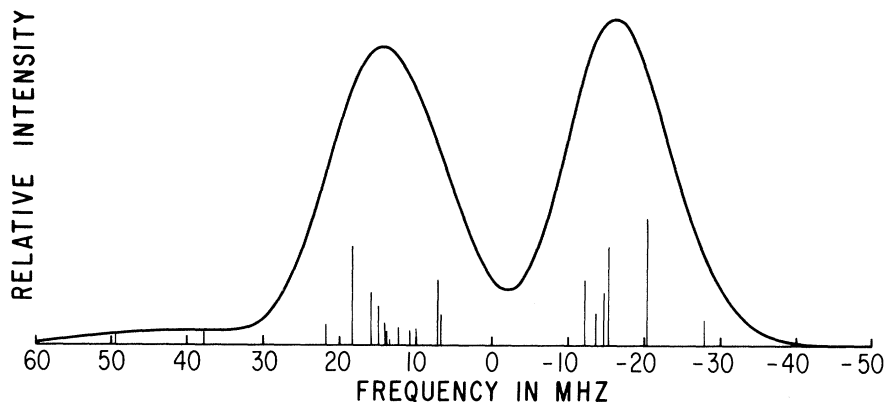


FIG. 1. Hyperfine structure of the $(1,1)-(0,2)$ transition of HD^+ . Note that the frequency increases to the left. This figure should be compared with Fig. 2 of Ref. 1.

experimental results prior to publication, and David M. Bishop for sending them the HD^+ potential-energy curve. One of us (P.R.C.) thanks the A. P. Sloan Foundation for a fellowship.

†This work was supported by National Science Foundation Grant No. CHE74-17494-A01.

¹W. H. Wing, G. A. Ruff, W. E. Lamb, Jr., and J. J. Spezeski, *Phys. Rev. Lett.* **36**, 1488 (1976).

²D. M. Bishop, *Phys. Rev. Lett.* **37**, 484 (1976).

³K. B. Jefferts, *Phys. Rev. Lett.* **23**, 1476 (1969).

⁴A. Dalgarno, T. N. L. Patterson, and W. B. Somerville, *Proc. Roy. Soc. London, Ser. A* **259**, 100 (1960).

⁵S. K. Luke, *Astrophys. J.* **156**, 761 (1969), and references contained therein.

⁶P. M. Kalaghan and A. Dalgarno, *Phys. Lett.* **38A**, 485 (1972).

⁷J. J. Tortorelli and J. E. Harriman, University of Wisconsin Theoretical Chemistry Institute Report No. WIS-TCI-456, 1971 (unpublished).

⁸D. M. Bishop and R. W. Wetmore, *J. Mol. Spectrosc.* **26**, 145 (1973).

Stability Limitations on High-Beta Tokamaks*

A. M. M. Todd, M. S. Chance, J. M. Greene, R. C. Grimm, J. L. Johnson,† and J. Manickam
Plasma Physics Laboratory, Princeton University, Princeton, New Jersey 08540

(Received 24 January 1977)

Magnetohydrodynamic instabilities limit the material that can be contained in a tokamak. The nature of the dangerous kink and ballooning modes is investigated for a typical configuration. In high-beta systems the most dangerous instabilities are ballooning modes that form large convective cells concentrated in regions of unfavorable magnetic field-line curvature.

The flux-conserving tokamak concept¹ has provided a prescription for choosing achievable plasma parameters when rapidly heating a plasma from an easily formed low-pressure configuration. It has been shown that equilibrium considerations do not provide an absolute limit to the maximum pressure that can be contained. Magnetohydrodynamic stability considerations provide such a limit. We study this problem numerically, using the PEST package,² by treating a series of equilibria that could be associated with the device³ being built at the Princeton University Plasma Physics Laboratory.

We choose as our starting point the equilibrium of Fig. 1. The pressure is proportional to $(\Psi_b - \Psi)^2$ with Ψ_b the poloidal flux at the plasma boundary. The safety factor $q \equiv d\Phi/d\Psi$, with Φ the toroidal flux, increases from 1.04 at the axis to 3.77 at the boundary. The plasma, with aspect ratio $R/a = 4.6$, where R is the distance from the major axis to the magnetic axis and πa^2 the cross-sectional area of the plasma surface, is supported by currents in external poloidal field coils that create a favorable field index throughout the plasma. The fusion-power-averaged pressure is

$$\beta^* = 2\mu_0 \left(\int p^2 dV / V \right)^{1/2} B_0^{-2} = 1.6\% \quad (1)$$

for this configuration. Other commonly used

pressure averages include

$$\bar{\beta} \equiv 2\mu_0 \int p dV / B_0^2 V = 1.0\%$$

and

$$\beta_p \equiv 4 \frac{\int p dV}{\int (I'V/V') d\Psi} = 2.1,$$

with I the toroidal current, V the volume, and B_0 the toroidal field. The difference between β^* and

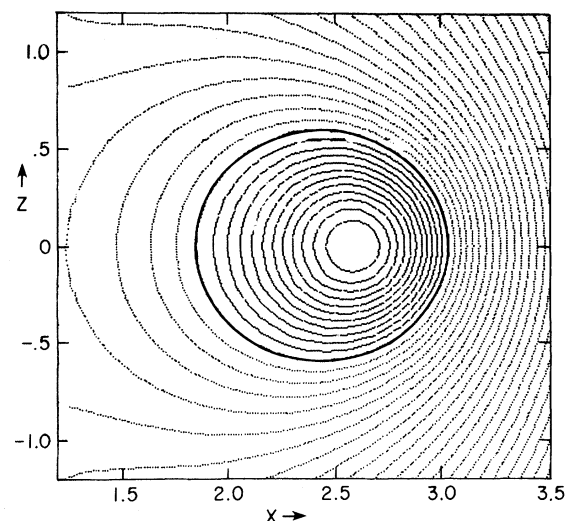


FIG. 1. Flux surfaces for a TFTR configuration with $\beta^* = 1.6\%$. The heavy solid curve is the plasma surface.